Ore Geology Reviews 90 (2017) 52–62

Contents lists available at ScienceDirect

Ore Geology Reviews

journal homepage: www.elsevier.com/locate/oregeorev

Micro-scale sulfur isotope and chemical variations in sphalerite from the Bleiberg Pb-Zn deposit, Eastern Alps, Austria

Elisabeth Henjes-Kunst[a,*], Johann G. Raith[a], Adrian J. Boyce[b]

[a] Montanuniversität Leoben, Chair of Resource Mineralogy, Peter Tunner-Straße 5, 8700 Leoben, Austria
[b] Scottish Universities Research Centre (SUERC), East Kilbride, Glasgow G75 0QF, Scotland, UK

ARTICLE INFO

Keywords:
Sphalerite
Carbonate hosted Pb-Zn deposits
In situ sulfur isotope analysis
Trace elements
Eastern Alps

ABSTRACT

The Bleiberg Pb-Zn deposit in the Drau Range is the type locality of Alpine-type carbonate-hosted Pb-Zn deposits. Its origin has been the subject of on-going controversy with two contrasting genetic models proposed: (1) the SEDEX model, with ore forming contemporaneously with sedimentation of the Triassic host rocks at about 220 Ma vs. (2) the epigenetic MVT model, with ores forming after host rock sedimentation at about 200 Ma or later. Both models assume that, on a deposit or even district scale, a fixed paragenetic sequence of ore minerals can be established. The results of our detailed petrographic, chemical and sulfur isotope study of two key ore-samples from two major ore horizons in the Wetterstein Formation at Bleiberg (EHK02 Erzkalk horizon and Blb17 Maxer Bänke horizon) demonstrate that there is no fixed paragenetic sequence of ore minerals. Small-scale non-systematic variations are recorded in textures, sphalerite chemistry and $\delta^{34}S$. In each sample, texturally different sphalerite types (colloform schalenblende, fine- and coarse-grained crystalline sphalerite) co-occur on a millimeter to centimeter scale. These sphalerites represent multiple mineralization stages/pulses since they differ in their trace element inventory and in their $\delta^{34}S$. Nonetheless, there is some correspondence of sphalerite micro-textures, sulfur isotope and chemical composition between the two samples, with microcrystalline colloform schalenblende being Fe-rich, having high Fe/Cd (15 and 9, respectively) and a light sulfur isotope composition ($\delta^{34}S$ −26.0 to −16.2‰). Cadmium-rich and Fe-poor sphalerite in both samples has relatively heavier sulfur isotope composition: in sample EHK02 this sphalerite has Fe/Cd of ~0.5 and $\delta^{34}S$ from −6.6 to −4.6‰; in sample Blb17 Fe/Cd is ~0.1 and $\delta^{34}S$ ranges from −15.0 to −1.5‰. Barite, which is restricted to sample EHK02, has $\delta^{34}S \approx 17$‰. The large variations in $\delta^{34}S$ recorded on the mm to cm-scale is consistent with variable contributions of reduced sulfur from two different sulfur reservoirs. The dominant reservoir with $\delta^{34}S$ values < −20‰ likely results from local bacteriogenic sulfate reduction (BSR), whereas the second reservoir, with $\delta^{34}S$ about −5‰ suggests a hydrothermal source likely linked with thermochemical sulfate reduction (TSR). Based on this small- to micro-scale study, no simple, deposit-wide paragenetic and sulfur isotope evolution with time can be established. In the Erzkalk ore (sample EHK02) an earlier Pb-Zn-Ba stage, characterized by heavy sulfur isotope values, is succeeded by a light $\delta^{34}S$-dominated Zn-Pb-F stage. In contrast, the several mineralization pulses identified in the stratiform Zn-Pb-F Maxer Bänke ore (sample Blb17) define a broad trend to heavier sulfur isotope values with time. The interaction documented in these samples between two sulfur reservoirs is considered a key mechanism of ore formation.

1. Introduction

Bleiberg (Austria) is the type locality of carbonate-hosted Alpine-Type (APT) Pb-Zn deposits. It was the largest and economically most important Pb-Zn deposit in the Alps. Together with other deposits like Mežica (Slovenia) it is part of an extensive historic mining district of stratabound Pb-Zn deposits hosted in the Early Mesozoic carbonate-dominated sedimentary sequences of the Drau Range in the Eastern Alps (Fig. 1a, b). The genesis of these Pb-Zn deposits has long been controversial, the spectrum of proposed genetic models ranging from syngenetic synsedimentary (e.g., Schulz, 1968) to epigenetic Mississippi-Valley Type (MVT) models (e.g., Leach et al., 2003).

Traditionally, Bleiberg has been interpreted as a distinct ore deposit type referred to as Alpine-Type Pb-Zn deposits (APT; Brigo et al., 1977; Köppel, 1983) and it has been considered distinct from the classic Mississippi-Valley Type (MVT) deposits due to its markedly different Pb isotope signature (Stanton and Russel, 1959) and other chemical criteria (Schroll, 1983; ; Schroll, 1996). A characteristic feature of APT

* Corresponding author.
E-mail addresses: e.henjes-kunst@gmx.at (E. Henjes-Kunst), johann.raith@unileoben.ac.at (J.G. Raith), a.boyce@suerc.gla.ac.uk (A.J. Boyce).

http://dx.doi.org/10.1016/j.oregeorev.2017.10.020
Received 10 October 2017; Accepted 23 October 2017
Available online 25 October 2017
0169-1368/ © 2017 Elsevier B.V. All rights reserved.

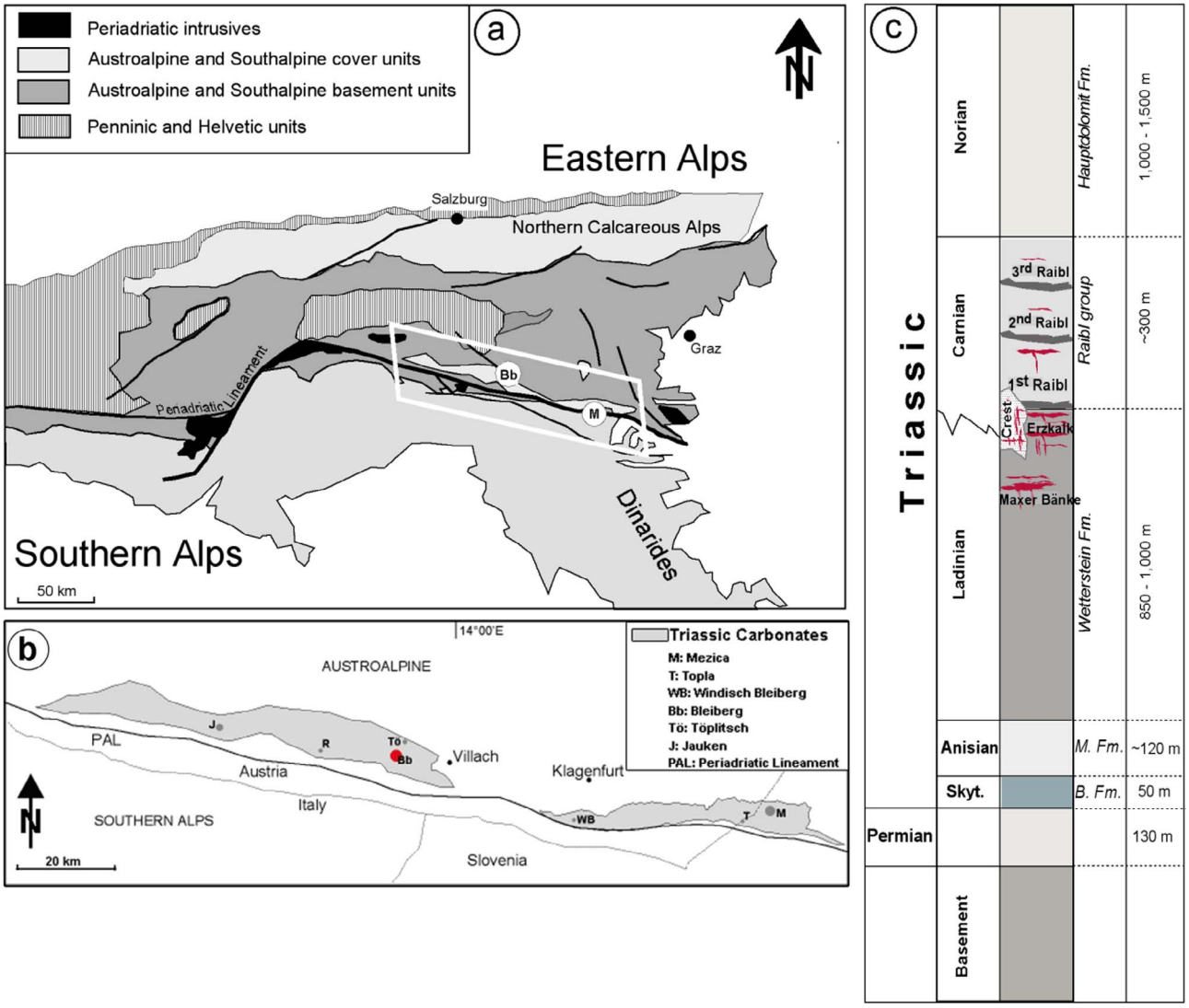

Fig. 1. a) Major units of the Alps, modified after Schroll and Rantitsch (2005). The white parallelogram marks the position of the Drau Range (Bb = Bleiberg, M = Mežica). b) Simplified sketch of the Drau Range and the location of some of the larger historic Pb-Zn deposits. c) Schematic stratigraphic profile of the Permomesozoic strata in Drau Range (B. Fm. = Buntsandstein Formation, M. Fm. = Muschelkalk Formation) with the position of the ore horizons at Bleiberg, simplified after Cerny (1989).

deposits is the very light sulfur isotope composition of ore sulfides, with $\delta^{34}S$ typically below −20‰ (Schroll et al., 1983; Leach et al., 2005; Schroll and Rantitsch, 2005); at Bleiberg more than 50% of the sulfides have $\delta^{34}S$ values below −20‰. This predominant, negative sulfur isotope signature indicates that open system bacterial sulfate reduction played a key role in providing reduced sulfur for sulfide formation (e.g., Schroll and Rantitsch, 2005; Kucha et al., 2010). However, there is also evidence for a second non-bacterial sulfur source at Bleiberg, characterized by less negative $\delta^{34}S$ values (about −10 to −1‰ $\delta^{34}S$), which is interpreted as input from a poorly characterized hydrothermal sulfur reservoir (Schroll and Rantitsch, 2005). Questions remain as to whether Pb-Zn mineralization occurred at different stages and at different times, with episodic input from two sulfur reservoirs, or if these sources mixed dynamically at the time of ore deposition and, if so, on what scale (Schroll, 2008).

We present results of a detailed investigation of two sphalerite ores from two major ore horizons (Erzkalk and Maxer Bänke) within the Wetterstein Formation at Bleiberg using a multi-analytical small-scale approach, in order to address these key questions. The samples were selected from a pool of about 70 samples studied in the PhD thesis by the first author (Henjes-Kunst, 2014) because the ore-gangue textures from these two horizons have been used to support the syngenetic model for APT deposits (e.g., Hagenguth, 1984; Schulz, 1968; Siegl, 1985). For each sample a specific crystallization sequence with time of ore and gangue minerals can be established. The focus was on sphalerite because it shows a considerable textural and chemical variation in carbonate-hosted ore deposits (Barrie et al., 2009; Pfaff et al., 2011). Combining chemical and sulfur isotope data of sphalerite with paragenetic information sheds new light on the dynamism of the mixing processes that operate in APT Pb-Zn deposits.

2. Geological setting and Pb-Zn mineralization

The Drau Range, where the Bleiberg deposit is located, extends over a distance of approximately 180 km, parallel to the Periadriatic Lineament, a prominent first order tectonic structure in the Alps (Fig. 1a, b). More than 100 Pb-Zn deposits and showings, mostly hosted in Triassic carbonate sequences, are known in the Drau Range (Fig. 1b). Similar carbonate-hosted Pb-Zn deposits are also widespread in the Northern Calcareous Alps and in the Southern Alps (Cerny, 1989).

A schematic stratigraphic profile (Upper Paleozoic – Mesozoic) is illustrated in Fig. 1c. In the Bleiberg area, the sediment cover (Permian to Mesozoic), resting unconformably on low-grade metamorphic pre-Mesozoic basement rocks, includes Triassic red beds (Scythian, Alpine

Buntsandstein Formation), shallow marine carbonate sequences (Anisian, Alpine Muschelkalk Formation), lagoonal and reef carbonate sequences (Ladinian to Carnian, Wetterstein Formation), carbonate-clastic sequences of the Raibl Group (Carnian) and lagoonal carbonate rocks (Norian, Hauptdolomit Formation). The limestones in the different formations are partly to completely dolomitized. This marine carbonate-dominated sedimentary sequence has been formed at a passive continental margin during the early stages of the development of the Tethys (Schroll, 1996).

Mining at Bleiberg started in the 14th century and terminated in 1992, extracting about 2.2 Mt of metal (approximately the same amounts of Pb and Zn, Schroll, 2008). The Pb-Zn ores are hosted by carbonate rocks of different lithofacies of Triassic age. Cerny (1989) distinguished six different ore horizons within the Ladinian/Carnian sedimentary units at Bleiberg (Fig. 1c): (1) The *Maxer Bänke*, the deepest ore horizon in the Wetterstein Formation, (2) the *Erzkalk* in the uppermost ~120 m of the Wetterstein Formation below the 1st Raibl shale, (3) the *Crest horizon*, which occurs in a similar stratigraphic position as the Erzkalk, but consists of a different lithofacies and (4), (5) and (6) Pb-Zn ores within the 1st, 2nd and 3rd carbonate interlayer, respectively, of the Raibl Group. Historically, the ore horizons in the Wetterstein Formation, especially the Erzkalk horizon within the Upper Wetterstein Formation, were most important regarding production of Pb and Zn.

The Maxer Bänke horizon was exclusively mined in the western part of the mine (total metal content 100,000 t of ore, Pb:Zn = 1:8, Weber, 1997). It is the deepest ore horizon at Bleiberg occurring 170–360 m below the 1st Raibl shale (Fig. 1c). The carbonate rocks hosting the Maxer Bänke ores were characterized by a highly irregular relief and variable microfacies from sub-, inter- to supratidal environments (e.g., oolite, mudstone, pelitic mudstone, grapestone; Hagenguth, 1984). Hagenguth (1984) reported Zn-Pb mineralization within dolomites (or marly dolomites) in all these environments. Mineralization within the subtidal sediments is typified by stratiform beds of fine-grained sphalerite (+ subordinate galena) and authigenic quartz. Mineralization in the intertidal facies is characterized by larger crystalline and colloform sphalerite (schalenblende) with common anhedral galena. In the supratidal facies mineralization is commonly discordant, e.g., schalenblende in cracks, which formed due to emersion (Hagenguth, 1984). Thus, the ores within the Maxer Bänke can be concordant as well as discordant, with stratiform ore bodies generally having a limited lateral extension.

Historically, Erzkalk was the most extensively mined ore horizon in the Bleiberg mine (total metal content 1.5 Mt of Pb and Zn; Pb:Zn = 1:1–1:4; Weber, 1997), and has been referred to as the "special facies" (in German "Sonderfazies", Holler, 1936). It comprises eight separate concordant ore horizons in the top 120 m of the Wetterstein Formation (Fig. 1c). Its lithofacies differs from that of the adjacent Wetterstein Formation by being deposited in a topographically elevated zone. It consists of cyclic alternating beds of sub-, inter- and supratidal sediments including emersion layers formed as the result of combined cyclic sea level oscillations and the relative topographic elevation of this zone with respect to the surrounding platform sediments (Bechstädt, 1975; Zeeh, 1994). The subtidal sediments are mainly composed of limestones and/or dolostones; the inter- to supratidal sediments are characterized by a rapid alternation of various lithologies like packstones, wackestones, mudstones and intercalated stromatolite layers. The emersion layers commonly occur above erosional unconformities and consist of caliche crusts and pisolites. Periodic emersion also facilitated meteoric karstification of the sediments (Bechstädt, 1979). Stratiform ores within the Erzkalk are generally restricted to such emersion layers and are rather small-scale with a volume of ~80 m^3 (Cerny, 1989). More broadly, however, stratiform ores in the Erzkalk, connected to emersion layers, can be traced over several kilometers of the deposit. In addition, discordant mineralization in veins or in irregular cavities is present. The timing and interplay of diagenetic versus hydrothermal dolomitization, which commonly accompanies the ores, are still unclear.

Stratiform ore textures, characterized by fine-grained alternating banding/laminations of ore and gangue minerals ("ore rhythmites") are typical of both the Maxer Bänke and Erzkalk. Several authors (Schneider, 1964; Schulz, 1968; Siegl, 1985) interpreted these textures as sedimentary and favored syngenetic exhalative precipitation of ore minerals directly on the seafloor (cf., SEDEX model). Alternatively, these rhythmites were interpreted as intra-karst sediments (Bechstädt, 1979; Leach et al., 2003).

Rubidium-Sr isochron dating of 15 mineral separates (sphalerite + Fe-sulfides) from different ore horizons in the western Bleiberg mine yielded two age groups (Melcher et al., 2010). The majority of sphalerite separates yielded a well-defined isochron age of 201 ± 1.6 Ma (n = 12); the second age of 225 ± 1.6 Ma is less well constrained (n = 3).

3. Samples and methods

3.1. Samples

The two samples selected for this study represent different lithofacis within the Wetterstein Formation and are from different ore horizons. Sample EHK02 is from the Erzkalk horizon from Antoni 6th level, Pflockschachtlager, from the central to western part of the Bleiberg mine; sample Blb17 is from Maxer Bänke horizon at Bellegarde-Schachtl from the western part of the Bleiberg mine. Sample EHK02 has been described as "cocade ore" (Schroll, 1983) typical for the Erzkalk horizon. Sample Blb17 comprises schalenblende aggregates and layers of fine-grained sphalerite. This fine-grained stratiform texture is characteristic of sphalerite ores from the Maxer Bänke horizon (Hagenguth, 1984). These two representative samples were chosen from a set of about 70 samples that were investigated during the PhD thesis of the first author (Henjes-Kunst, 2014) and selected because of the visible micro-textural similarities (e.g., schalenblende) and potential presence of several mineralization stages within each sample. Petrographic characteristics of these two samples were studied in detail using standard optical microscopy (transmitted and reflected light) focusing on textures and paragenetic ore-gangue relationships.

3.2. Mineral chemical analyses

Mineral chemical analyses of sphalerite were performed using the Cameca SX100 electron microprobe (EPMA) at the Federal Institute for Geosciences and Natural Resources (BGR) in Hannover (Germany) and the Jeol JXA8200 instrument of Universitätszentrum Angewandte Geowissenschaften Steiermark at the Chair of Resource Mineralogy, Montanuniversität Leoben (Austria). Both instruments operated in the wavelength dispersive (WDS) mode. During EPMA sessions the concentrations of As, Fe, Pb, Ge, Cu, Tl, Cd and Zn and S in sphalerites were analyzed. Analytical conditions and limits of detection are reported in Table 1. The mineral chemical data set of the Jeol JXA8200 is provided as electronic Supplementary material to this paper (Online Resource 1).

3.3. QEMSCAN

Quantitative mineral and textural analysis was done by automated scanning electron microcopy (QEMSCAN, **Q**uantitative **E**valuation of **M**inerals by **Scan**ning electron microscopy) on polished thin sections of 30 μm thickness. The analyses were made at FEI laboratories in Brisbane, Australia (analysts Leonardo Salazar and Gerda Gloy) using a FEI Quanta 650F SEM instrument equipped with two Bruker EDS detectors and the QUEMSCAN software. The analyses were carried out in the FieldImage mode. In order to illustrate the delicate differences in the ore-gangue assemblages the samples were scanned automatically using 10 and 5 μm spot sizes, respectively. The results are shown in

Table 1
Analytical conditions and standards used for EMP analyses in the microprobe laboratories at BGR Hannover (Cameca SX100) and Montanuniversitaet Leoben (Jeol JXA8200).

	CAMECA SX100 (30kV, 40nA)					JEOL JXA8200 (20 kV, 40nA)				
	Line	Crystal	Time P/BG	Standard	Approx. LoD [ppm]	Line	Crystal	Time P/BG	Standard	Approx. LoD [ppm]
S	Ka	PET	10/5	ZnS	400	Ka	PETJ	15/5	ZnS	80
Zn	Ka	LLIF	10/5	ZnS	560	Ka	LIFH	15/5	ZnS	130
Fe	Ka	LLIF	30/15	FeS	100	Ka	LIFH	20/10	$CuFeS_2$	50
Cd	La	PET	120/60	Cd	240	La	PETH	90/40	Cd	30
Pb	Ma	PET	10/5	PbS	2000	Ma	PETJ	20/10	PbS	250
Ge	Ka	LLIF	120/60	Ge	130	La	TAP	90/40	Ge	40
As	La	TAP	140/70	AsGa	250	La	TAP	90/40	PtAs	50
Cu	Ka	LLIF	130/75	Cu	110	Ka	LIFH	90/40	$CuFeS_2$	60
Tl	Ma	LPET	140/70	Tl	670	Ma	PETH	90/40	TlBrI	300

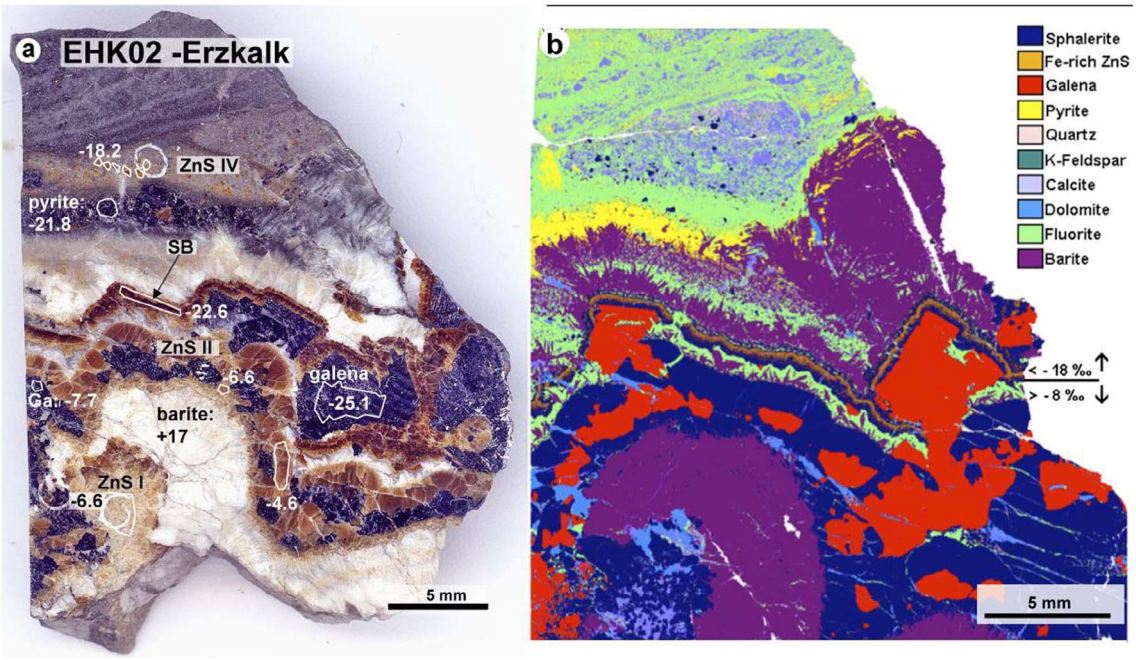

Fig. 2. a) Polished block of sample EHK02. The notation of the different sphalerite types is explained in the text. b) QEMSCAN color-coded mineral map of polished thin section prepared from the counter-piece of the polished block shown in a. See text for detailed explanations.

color-coded mineral maps in comparison with photographs of the two samples (Figs. 2a, b and 3a, b). The modal mineralogical composition (Table 2) was calculated from QEMSCAN data.

3.4. Sulfur isotope analyses

For sulfur isotope analyses, polished blocks (approximately 2 × 3 cm in size, Figs. 2a and 3a) were prepared from counter-pieces of the slabs, which were taken for preparation of the polished thin sections. Full mineralogical and textural characterization of the samples was performed prior to the isotope analyses.

All sulfur isotope analyses were performed at the Scottish Universities Environmental Research Centre (SUERC). Sulfur isotope analyses were carried out by conventional and *in situ* laser extraction. Conventional analyses were carried out on micro-drilled powders (area affected by the driller is at least 1 mm wide and 5 mm long) combusted by the standard procedure of Robinson and Kusabke (1975) for sulfides and Coleman and Moore (1978) for barites.

In situ laser combustion was carried out using the method described in Fallick et al. (1992) and Wagner et al. (2002). All data are presented as true $\delta^{34}S$, corrected using the small mineral-dependent laser fractionation factors calculated by Wagner et al. (2002). Pure SO_2 gases delivered by each of these techniques were analyzed either on-line to a VG SIRA II (laser), or Thermo Fisher Scientific MAT 253 (conventional) mass spectrometer. Raw machine $\delta^{66}SO_2$ data were converted to $\delta^{34}S$ by calibration with international standards NBS-123 (+17.1‰) and IAEA-S-3 (−31.5‰), as well as SUERC's internal lab standard CP-1 (−4.6‰). Reproducibility of the analytical results (around ± 0.2‰ during these analyses) was controlled through replicate measurements of these standards. All sulfur isotope compositions were calculated relative to Vienna Canon Diablo Troilite (V-CDT) and are reported in standard permil notation.

4. Results

4.1. Petrography

4.1.1. EHK02 – Erzkalk horizon

Sample EHK02 consists of sphalerite, galena and minor amounts of pyrite. The gangue is composed of barite, calcite, dolomite, fluorite and quartz (Fig. 2a, b; Table 2). Textural relationships indicate that several generations or types of sphalerite and the ore/gangue paragenesis formed sequentially, perhaps related to mineralization pulses (from the bottom to the top as shown in Fig. 2a, b). The four sphalerite "types" distinguished (i.e. EHK02_ZnS I, EHK02_ZnS II; EHK02_SB and EHK02_ZnS IV) are described as follows:

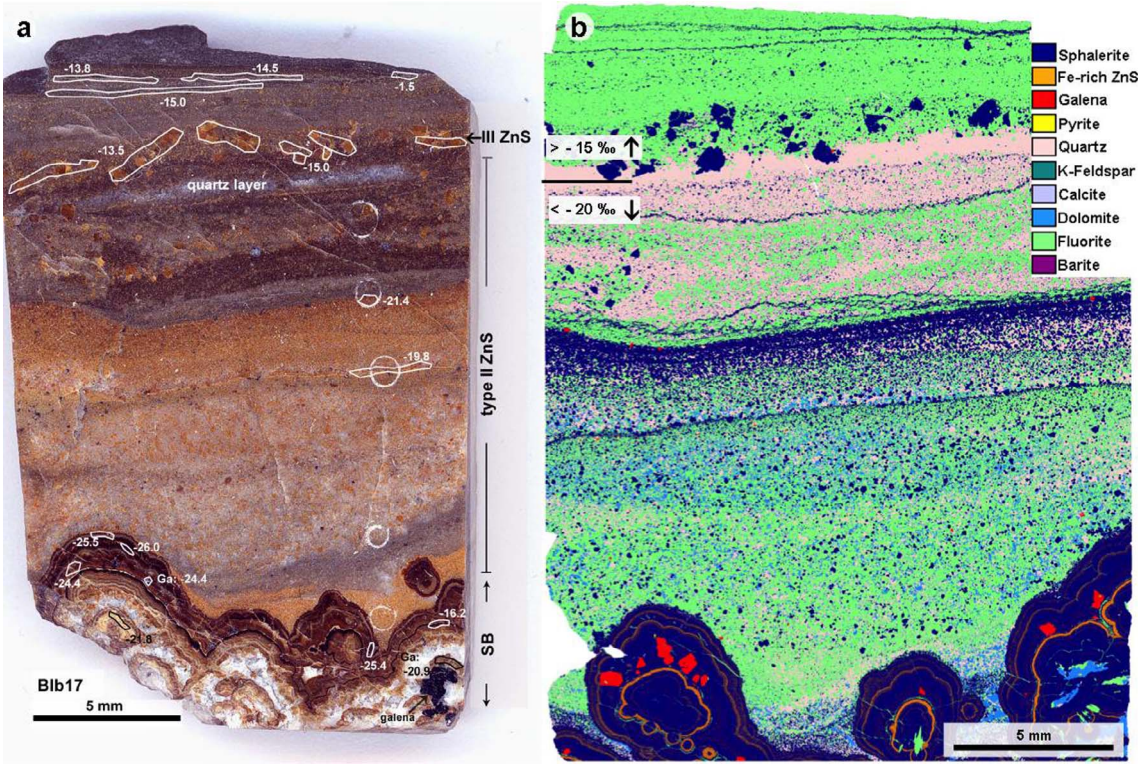

Fig. 3. a) Polished block of sample Blb17. The notation of the different sphalerite types is explained in the text. b) QEMSCAN color-coded mineral map of polished thin section prepared from the counter-piece of the polished block shown in a. See text for detailed explanations.

Table 2
Modal mineralogical composition (vol%) of samples EHK02 and Blb17 calculated from QUEMSCAN analyses.

Mineral	vol%	
	EHK02	Blb17
Sphalerite	24.6	30.9
Fe-rich sphalerite	1.2	2.2
Galena	22.8	0.9
Pyrite	3.6	0.0
Quartz	1.0	19.6
K-Feldspar	0.3	0.9
Calcite	4.5	1.4
Dolomite	1.0	4.9
Fluorite	11.5	38.2
Barite	28.9	0.0
Other	0.7	0.9
Total	**100.0**	**100.0**

- EHK 02_ZnS I, a pale beige, crystalline sphalerite (a few 100 μm in size), intimately inter-grown with calcite, is the paragenetically oldest mineralization. This sphalerite is overgrown by a band composed of coarse anhedral barite and galena and crosscut by dolomite veinlets.
- EHK02_ZnS II is a coarse grained (up to 2 mm), pale beige sphalerite-dominated band. Subsequent to its formation, a barite band occurs (similar grain size barite associated with EHK02_ZnS I) followed by euhedral galena (Fig. 2a).
- EHK02_SB is a sphalerite band, about 800 μm thick, showing characteristic schalenblende texture (i.e. alternate colloform banding on the micro-scale) consisting of four slightly differently colored microcrystalline sphalerite layers. This schalenblende clearly overgrows the euhedral galena associated with EHK02_ZnS II. Subsequently a mixture of barite and fluorite was precipitated, followed by pyrite.
- EHK02_ZnS IV is the youngest sphalerite and forms fine-grained (approximately 100 μm) grayish-brown crystals that post-date pyrite. This sphalerite is inter-grown with carbonates (calcite, dolomite) and fluorite. The top part of the sample is free of barite and dominated by fluorite showing a laminated fabric (Fig. 2a, b). The lamination is caused by varying contents of fluorite, carbonate minerals and quartz.

The whole sample, especially in its bottom part, shows some late brittle deformation. Micro-fractures are mostly filled with dolomite (Fig. 2b). The texture of this sample suggests formation due to episodic precipitation of sphalerite, galena and the gangue minerals within a cavity. Regarding the distribution of the gangue phases, two main paragenetic stages are clearly distinguished: In the lower part barite and carbonates are the exclusive gangue minerals, whereas in the upper part fluorite becomes the dominant gangue mineral. There, fluorite is associated with calcite, dolomite and quartz but without barite. As will be seen below, these petrographic differences are also reflected in the sulfur isotope and chemical composition of the sphalerites.

4.1.2. *Blb17 – Maxer Bänke horizon*

The mineral assemblage of sample Blb17 consists of sphalerite and galena, with a predominance of sphalerite (Fig. 3a, b, Table 2). The gangue is primarily composed of fluorite and subordinate quartz and dolomite. Quartz is especially enriched in the upper third of the sample, where it forms a nearly mono-mineralic quartz layer with a sharp upper contact, above which quartz is rare (Fig. 3b).

Three main textural varieties of sphalerite (Blb17_SB, Blb17_ZnS II, Blb17_ZnS III) can be distinguished in this sample (from bottom to top in Fig. 3a), with Blb17_SB representing the earliest formation stage and Blb17_ZnS III the latest one.

- Blb17_SB consists of an up to ≤0.5 cm thick polycrystalline schalenblende aggregate of variably colored microcrystalline sphalerite bands. Galena occurs in accessory amounts, forming near euhedral

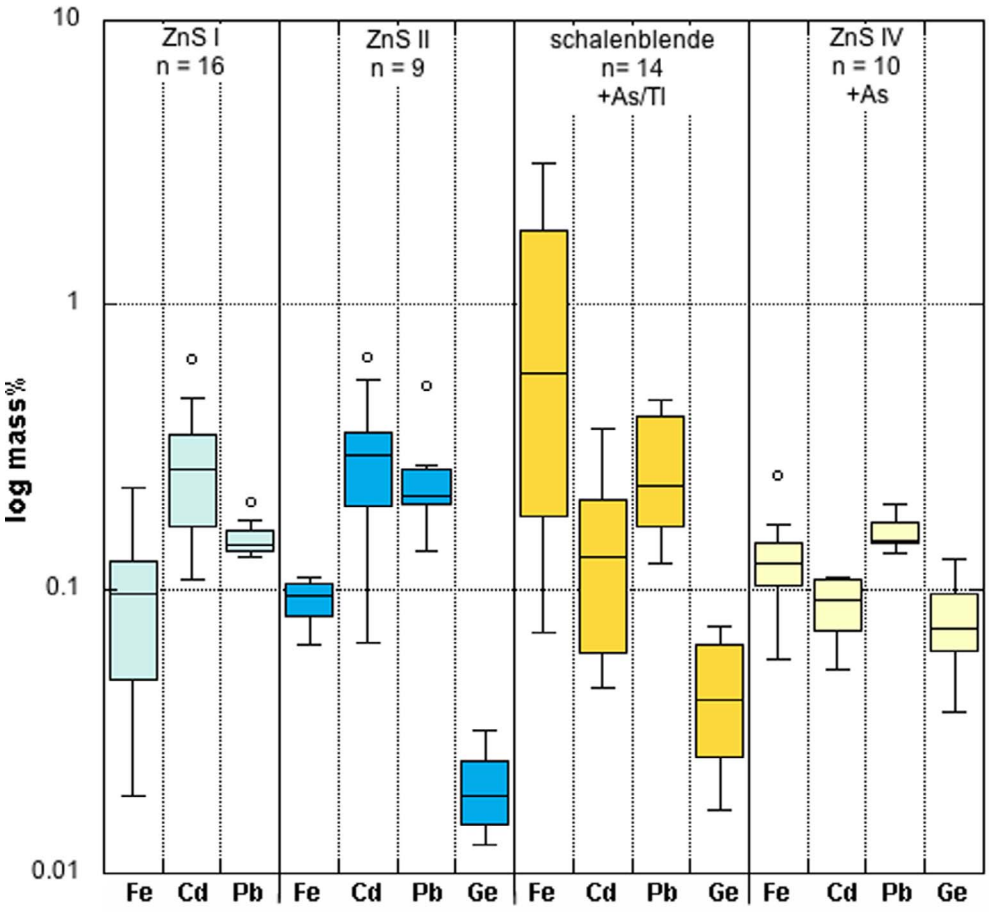

Fig. 4. Boxplots showing the distribution of some trace/minor elements in sphalerite in sample EHK02 - Erzkalk. Sphalerite notation as in Fig. 2 a. I = EHK02_ZnS I, II = EHK02_ZnS II, etc.

crystals within the schalenblende.

- Blb 17_ZnS II comprises fine-grained sphalerite, arranged in discrete layers with fluorite and minor quartz defining a rhythmic layering. Individual layers are characterized by sphalerite crystals of certain grain size and color and different modal proportions of the minerals, and the layers have the appearance of sedimentary banding.
- Blb 17_ZnS II comprises coarser-grained (~500–2000 μm) subhedral brownish sphalerite grains in the uppermost part of the sample, where it occurs from the contact of the quartz-rich to the quartz-free layer.

In the bottom part of the sample the layering partly follows and infills depressions on the convex boytroidal surface of the schalenblende (Fig. 3a, b), which confirms that the sequence is younging-up towards the top of the photograph. This is also consistent with the preferred convex growth direction of schalenblende (Roedder, 1968). These discrete finely layered textures strongly suggest that the ore was precipitated in distinct pulses.

4.2. Chemical composition of sphalerite

The results of EPMA analyses on sphalerite are summarized in boxplots (Fig. 4). Representative analyses are listed in Online Resource 1 as supplementary electronic material. Iron and Cd are nearly omnipresent in all sphalerites and show the highest concentrations among the analyzed minor/trace elements in sphalerite. Hence, we used the Fe/Cd to document the chemical variance among the various sphalerite types.

Schalenblende (SB, yellow boxes) is characterized by variable, but relatively high Fe contents ranging between 700 ppm and 3.2 mass% Fe (mean 9700 ppm), with a dark brown schalenblende layer in the central part that is particularly Fe-rich (shown as Fe-rich sphalerite on Fig. 2b). Cadmium contents of this sphalerite type are between 500 and 3700 ppm (mean 1600). The average Fe/Cd of this schalenblende is 14.8 (Table 4). One analysis of this sphalerite type revealed 830 ppm Tl. The beige EHK02_ZnS II aggregate (dark blue boxes in Fig. 4) shows lower Fe concentrations (600–1000 ppm, mean 900 ppm), but is higher in Cd (8600–6500 ppm, mean 3000 ppm) than the schalenblende resulting in considerably lower Fe/Cd of 0.5 (Table 4). The earliest sphalerite stage (EHK02_ZnS I; light blue boxes in Fig. 4) has a very similar trace element composition to the adjacent EHK02_ZnS II. It is also low in Fe and high in Cd (Fe/Cd = 0.5). In contrast EHK02_ZnS IV

Table 3
Results of sulfur isotope measurements.

EHK 02		Blb17	
Mineral/ZnS type	$\delta^{34}S$ [‰]	Mineral/ZnS type	$\delta^{34}S$ [‰]
type I ZnS	−6.6	SB	−21.5
type II ZnS	−6.6	SB	−16.2
type II ZnS	−4.6	SB	−25.4
galena	−7.7	SB	−24.4
galena	−25.1	SB	−26.0
SB	−22.3	SB	−25.0
SB	−22.6	galena	−20.9
pyrite	−21.8	galena	−24.4
type IV ZnS	−18.2	type II ZnS	−19.8
barite	+17.0	type II ZnS	−21.4
		type III ZnS	−15.0
		type III ZnS	−13.5
		type III ZnS	−15.0
		type III ZnS	−14.5
		type III ZnS	−13.8
		ZnS	−1.5

Table 4
Sphalerite types distinguished in samples EHK02 and Blb17. The relative chronology (old to young) and info about sphalerite texture, gangue paragenesis, Fe/Cd ratios of sphalerite and results (mean values) of sulfur isotope measurements are shown. Arrows in front of element symbol in the last column give qualitative information about element concentrations: arrow up = high, arrow down = low, arrow side up = moderately high.

EHK02, Bleiberg Erzkalk

Time	ZnS	Texture	Ore + gangue	$\delta^{34}S$	Fe:Cd	Trace/minor elements
old	I	coarse-grained ZnS accumulations	barite, calcite	−6.6	0.5	↑Cd ↓Fe
	II	coarse-grained ZnS accumulations	barite, secondary dolomite, anhedral galena	−7.7 to −4.6	0.5	↑Cd ↓Fe, Ge
young	SB	colloform schalenblende	fluorite, barite, euhedral galena	−22.6	14.8	↑Fe, Pb + ↗As, Tl, Ge ↓Cd
	IV	anhedral and fine-grained ZnS	fluorite, dolomite, pyrite	−18.6	1.6	↗Fe, Pb; ↑Ge ↓Cd

Blb17, Bleiberg Maxer Bänke

time	ZnS	texture	ore + gangue	$\delta^{34}S$	Fe:Cd	trace/minor elements
old	SB	colloform schalenblende	fluorite, dolomite, quartz + galena	−26 to −16.2	8.6	↑Fe, Pb, As + ↗Tl, Ge ↓Cd
young	II	fine-grained ZnS, partly enriched in II layers	fluorite, quartz, dolomite	~ −20	3.6	↗Fe, Pb, As, Ge ↓Cd
	III	coarse-grained ZnS + fine-grained ZnS	quartz, fluorite	−14 to −1.5	0.1	↑Cd ↓Fe, Ge

(light yellow boxes in Fig. 4) contains more Fe than EHK02_ZnS I/_ZnSII, but less than the schalenblende. The Cd concentrations of this latest formed sphalerite are generally low (EHK02_ZnS IV; average Fe/Cd = 1.6; Table 4). The difference between the two later sphalerite generations (schalenblende and EHK02_ZnS IV) and the two earlier formed sphalerite generations (EHK02_ZnS I/_ZnS II) is also seen in the As and Ge concentrations. The later sphalerite types usually contain detectable As (> 300 ppm) whereas in early ones As concentrations were only sporadically above detection limit of the microprobe. Germanium concentrations show also some systematic variation from EHK02_ZnS I to EHK02_ZnS IV. In both early-formed sphalerite types Ge was typically < 0.03 mass% or even below the limit of detection (e.g., in EHK02_ZnS I), whereas Ge contents in both later sphalerite types are usually > 0.03 mass%.

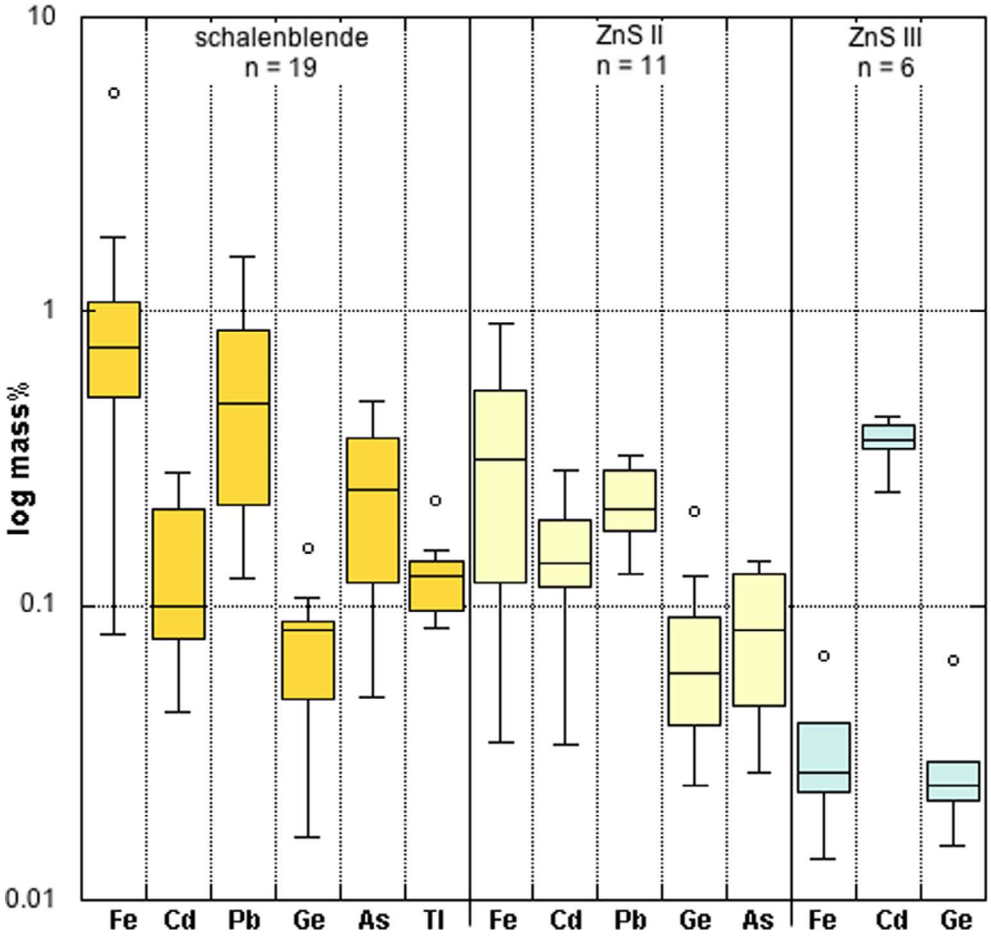

Fig. 5. Boxplots showing the distribution of some trace/minor elements in sphalerite in sample Blb17 - Maxer Bänke (SB = schalenblende; II = Blb17_ZnS II; III = Blb17_ZnS III). Elements, which are not displayed, were mostly below the detection limit of the EPMA.

4.2.1. Blb17 – Maxer Bänke horizon

The trace element characteristics of the three main sphalerite types in this sample are displayed as boxplots in Fig. 5. Iron contents in the schalenblende are very variable but are on average high (800 ppm – 5.6 mass%, mean 1 mass%), with individual layers within the schalenblende occasionally showing very high Fe contents (see also Fig. 3b). The Cd concentrations of the schalenblende are generally low ranging from 400 to 2800 ppm (mean 1400 ppm) resulting in an average Fe/Cd ratio of 8.6 (Table 4). The Fe contents of the Blb17_ZnS II range from 300 to 9000 ppm and are thus highly variable (mean 3600 ppm), but in general lower than in the schalenblende. The average Fe/Cd of Blb17_ZnS II is 3.6. The coarse-crystalline sphalerite Blb17_ZnS III and fine-grained sphalerite in the layers above (Fig. 3a, b) are characterized by low concentrations and limited variability in Fe (100–700 ppm, mean 350 ppm). Cadmium shows an opposite trend and is higher (2400–4400 ppm, mean 3600 ppm). Thus, the average Fe/Cd ratio of this sphalerite is very low (0.1). Besides the differences in the Fe/Cd of the three sphalerite types minor differences in As, Pb and Tl concentrations are documented. Both early-formed sphalerite types (Blb17_SB and Blb17_ZnS II) sometimes have Tl contents above the detection limit of the microprobe, and are often richer in Pb and As (Fig. 5; Online Resource 1).

4.3. Sulfur isotope data

Results of sulfur isotope analyses are listed in Table 3. The spatial distribution of sulfur isotope data within the two studied samples is illustrated in Figs. 2a and 3a.

4.3.1. EHK02 – Erzkalk horizon

The sulfur isotope composition of sphalerite is very heterogeneous with $\delta^{34}S$ between −4.6 and −22.6‰ (n = 9). Galena displays also a similar range from −25.1‰ to −7,7 (n = 2). Pyrite has a $\delta^{34}S$ of −21.8‰ and barite +17‰.

There is a clear and sudden change of about 17‰ over a distance of 5 mm (Fig. 2a), with earlier formed EHK02_ZnS I and EHK02_ZnS II (bottom part of the sample) being distinctly less negative (> −8‰ $\delta^{34}S$) than the later formed schalenblende and crystalline sphalerite ($\delta^{34}S$ = −22.6 to −18.2‰; central and top part in Fig. 2a). The $\delta^{34}S$ values of coexisting sphalerite-galena increase in accordance with the fractionation sequence of isotopic equilibrium (Ohmoto and Rye, 1979; Ohmoto, 1986), that is, PbS < ZnS. However, temperature calculations for EHK02 based on the $\Delta^{34}S$ values of sphalerite-galena pairs yielded unrealistic depositional temperatures (300–590 °C), which are far above the typical formation temperatures of carbonate-hosted Pb-Zn deposits (60–150 °C, rarely up to 250 °C, Ridley, 2013). Clearly, the two sulfides did not form in isotopic equilibrium.

4.3.2. Blb17 - Maxer Bänke horizon

Heterogeneity in $\delta^{34}S$ is also typical for this sample (Fig. 3a). The two early formed sphalerite types (Blb17_SB and Blb17_ZnS II) are dominated by light $\delta^{34}S$ (mostly < −20‰). The schalenblende itself exhibits some non-systematic variations in $\delta^{34}S$, with the least negative value (−16.2‰) measured on the thin Fe-rich layer in the center of the sample (Fig. 3a, b). In the youngest sphalerites (Blb17_ZnS III) a significant increase in $\delta^{34}S$ is visible (−15.0 to −13.5‰). The very fine-grained (~10 µm) top layer gave the isotopically heaviest $\delta^{34}S$ of −1.5‰. Unfortunately, only very small amounts of this layer were present in this sample, thus this sulfur isotope measurement could not be replicated.

Again, this sample records significant, although less dramatic, changes in sulfur isotope composition on the millimeter scale. To summarize: (a) The variation between individual layers of the schalenblende is ~10‰; (b) an abrupt change of about 5–6‰ occurs across the quartz-rich layer, and (c) there is a change of ~13‰ between adjacent layers with fine-grained sphalerite at the top of the sample.

4.4. Correlation of sphalerite chemistry and sulfur isotope composition

As documented above, texturally and chemically different sphalerite types are present in both samples though these textures are partly similar; for example, in each sample schalenblende aggregates are present. However, schalenblende formed at different times (relatively early vs. late) in the two samples and its associated ore and gangue minerals are neither texturally, nor chemically comparable. It is therefore highly unlikely that schalenblende formed during a *single* deposit (or ore horizon) spanning mineralization event. We were thus not able to establish a uniform paragenetic mineralization sequence valid for the Bleiberg deposit, let alone the whole Drauzug Pb-Zn district, as had been suggested by previous studies (e.g., Kuhlemann, 1995; Schroll, 1996; Zeeh, 1994). Our naming of the sphalerite types here therefore refers only to the within sample-scale formation stages.

In Table 4 sphalerite textures, qualitative trace/minor element concentrations, sulfur isotope composition and (gangue) mineralogy are compiled for each of the two samples in relation to its crystallization sequence. Fig. 6 illustrates the relation between the mean Fe/Cd ratios and the sulfur isotope composition of the different sphalerite types within each sample. Sphalerites with comparable texture, chemical and sulfur isotope composition occur in both samples but they show opposite evolution trends with time.

EHK02 – Erzkalk: The early formed EHK02_ZnS I has high Cd, but low Fe contents and a heavy sulfur isotope composition ($\delta^{34}S$ −6.6‰). The beige EHK02_ZnS II aggregates display a similar Fe/Cd distribution and heavy sulfur isotope composition ($\delta^{34}S$ −4.6 to −6.6.‰), with low or undetectable Ge contents. The gangue of EHK02_ZnS I and EHK02_ZnS II is mainly barite with small amounts of calcite the barite having $\delta^{34}S$ of + 17‰. Dolomite is restricted to late brittle structures

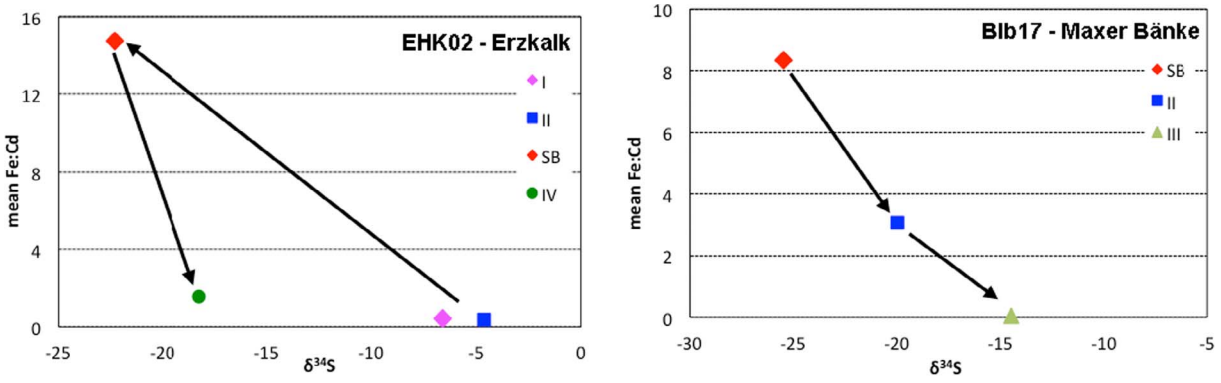

Fig. 6. Average Fe/Cd vs. $\delta^{34}S$ values of the different sphalerite types in samples EHK02 - Erzkalk and Blb17 - Maxer Bänke. Arrows indicate evolution from older to younger sphalerite types with each sample.

(Fig. 2b). The schalenblende (EHK02_SB) is characterized by a sudden increase in Fe and decrease in Cd, and a sudden decrease in $\delta^{34}S$ values to about −23‰. Additionally, it is relatively enriched in Pb, As, Ge, and sporadically Tl. The occurrence of schalenblende is furthermore marked by an obvious change in gangue mineralogy with fluorite becoming important. The late EHK02_ZnS IV has $\delta^{34}S$ of −18.2‰ and contains more Fe and less Cd than EHK02_ZnS I/ZnS II. The low Fe contents in EHK02_SB are accompanied by relative enrichment in Ge. The gangue in this top part of the sample is completely different; i.e., it is free of barite and fluorite coexists with dolomite. In addition, pyrite is present in discrete layers with a similar light $\delta^{34}S$ (−21.8‰).

Blb17 – Maxer Bänke: Schalenblende, the earliest phase in this sample, shows a generally light and variable sulfur isotope composition (−26 to −16‰ $\delta^{34}S$) and is characterized by high Fe and rather low Cd contents. Furthermore, it has high Pb and As and increased Tl and Ge concentrations. In the Blb17_ZnS II the Fe, Pb and As contents are lower than in the schalenblende while $\delta^{34}S$ remains enriched in ^{32}S (−20‰); Cd contents are low, whereas Ge contents are similar. The main gangue mineral of the two early sphalerite stages is fluorite, with minor amounts of dolomite and quartz. Blb17_ZnS III shows a sudden decrease in Fe concentrations, whilst Cd increases. This dramatic change (Fe/Cd = 0.1) is combined with an increase in $\delta^{34}S$ value to about −14‰. The gangue of Blb17_ZnS III consists solely of fluorite. The formation of the first coarse-grained Blb17_ZnS III layer is preceded by the precipitation of large amounts of quartz, which is subsequently completely absent (Fig. 3b).

Making some general observations, we note that in both samples, schalenblende has a high Fe/Cd and tends to be isotopically lighter than other sphalerite types. In contrast, crystalline sphalerite tends to have lower Fe and higher Cd contents (i.e. low Fe/Cd) and heavier sulfur in both samples, markedly in EHK02_ZnS I. Less distinct correlations exist between the Pb, As and Tl contents and the sulfur isotope composition of the sphalerite, although higher values are noted in the colloform schalenblende.

5. Discussion

5.1. Source of sulfur in Alpine type Pb-Zn deposits

Previous sulfur isotope studies on Alpine type Pb-Zn deposits in the Drau Range have already reported the large variability in the sulfur isotope composition (Herlec et al., 2010; Kuhlemann et al., 2001; Schroll et al., 1983; Schroll and Rantitsch, 2005). At Bleiberg, the $\delta^{34}S$ values of sphalerites from the six different ore horizons are in the range of −26 to −1‰ (Schroll and Rantitsch, 2005). Recently published sulfur isotope data on sphalerite from Bleiberg extended the sphalerite data set to $\delta^{34}S$ values down to less than −30‰ and confirmed the non-uniform distribution of the sulfur isotope data of sphalerites in the Bleiberg deposit (Kucha et al., 2010; Henjes-Kunst et al., 2013). Schroll and Rantitsch (2005) have distinguished three $\delta^{34}S$ populations at Bleiberg: one pronounced population at −25 to −29‰, a second one at −6 to −8‰ and a poorly defined third one with values in between. Schroll and Rantitsch (2005) interpret the sulfur isotope variation in sulfides from Bleiberg to reflect at least two different sulfur reservoirs and two different processes causing sulfate reduction; bacterial (BSR) vs. thermochemical sulfate reduction (TSR, Machel et al., 1995). The dominant population with very negative sulfur isotope compositions of sulfides (< −18‰) is linked with bacterial sulfate reduction (BSR), probably near the site of ore deposition, given the open system behavior reflected in the isotopic values (Schwarcz and Burnie, 1973). The population with heavier $\delta^{34}S$ values (−8 to 0‰) is interpreted as a hydrothermal or deep-seated sulfur reservoir derived via thermochemical sulfate reduction (TSR). Intermediate values are then explained as a mixing of these two end-members. Our data can be interpreted in this established framework. A novel aspect of the present study, however, is that we show that this variability is not only a feature on the regional and ore deposit scale, but even exists on the millimeter to centimeter scale, reflecting the dynamism of the ore forming process at hand specimen scale.

Based on sulfur isotope data of sulfides from the Drau Range Kuhlemann et al. (2001) proposed the presence of two paragenetic stages of Pb-Zn mineralization, which generally follow a trend towards heavier $\delta^{34}S$ values with time. A similar trend with time was observed by Herlec et al. (2010) for sulfide ores from the Mežica deposit. On the contrary, Schroll et al. (1983) proposed a temporal evolution towards lighter $\delta^{34}S$ values. Our data clearly demonstrate the presence of both trends in sulfur isotope evolution, even on the sample scale. Thus, our results contradict the previous attempts (Kuhlemann, 1995; Schroll, 1996; Zeeh, 1994) to establish a uniform paragenetic sequence for Pb-Zn mineralization in the Drau Range.

5.2. Evidence for mixing and multiple mineralization pulses

Fluids are necessary for the transport of sulfur (in the form of various aqueous species with different valence) and (base) metals towards the depositional site(s) in carbonate hosted Pb-Zn deposits. There are still some controversies regarding the question whether these fluids are capable of transporting base metals and sulfur at the same time and what the Pb and Zn complexing ligands are (e.g., Anderson, 1975; Sicree and Barnes, 1996). Also, the experimental work of Bischoff et al. (1981) shows that a significant reduced sulfide component can only be transported together with Pb and Zn (as chloride complexes) well above 200 °C. In the following we therefore argue that Pb-Zn mineralization at Bleiberg clearly formed by interaction of different fluids and that sulfur must have been provided from two different reservoirs.

The simplest explanation of the early Zn-Pb-Ba mineralization in sample EHK02 is that it formed whilst the system was dominated by sulfur from a (higher temperature? TSR?) hydrothermal reservoir, with $\delta^{34}S$ values around −6‰. This hydrothermal sulfur signature is correlated with an enrichment of Cd, what has also been seen in other studies of colloform and crystalline sphalerite (Barrie et al., 2009; Pfaff et al., 2011). We note that its association with a distinct barite-rich layer, which has $\delta^{34}S$ similar to Triassic seawater (i.e. +17‰, Table 3; Kampschulte and Strauss, 2004), suggests that the cavities into which the hydrothermal fluid ingressed likely contained seawater. In such circumstances, the barite forms through interaction of hydrothermal Ba with seawater sulfate upon mixing, a feature typical in some carbonate-hosted deposits (e.g. Ireland; Coomer and Robinson, 1976).

The sudden changes in texture, chemistry, $\delta^{34}S$ and gangue mineralogy in the upper half of sample EHK02 indicate an abrupt change of the physico-chemical conditions at the depositional site. Now the system becomes dominated by bacteriogenic sulfur and the limited hydrothermal sulfur reservoir is likely exhausted. It is likely that a second fluid contributed bacteriogenic sulfur, which was formed via BSR in an ± open system (shallow reservoir with sufficient supply of fresh seawater) and mixed with the metal bearing fluid. With this mineralization phase we note a very significant increase in Fe content of sphalerite, and to a limited extend also of Pb, As and Tl. Similar changes in sulfur isotope composition and trace element composition have been found in sphalerite in the carbonate-hosted MVT deposit Wiesloch, SW Germany (Pfaff et al., 2011).

In sample Blb17 a different sequence is documented. Mineralization starts with precipitation of schalenblende, which, as in the Erzkalk sample, is dominated by bacteriogenic sulfur. Again Pb, As and Tl are found at increased tenor, along with strong enrichment in Fe. Mixing between spent ore fluid (with respect to hydrothermal sulfide, but not metals) and a fluid containing the bacteriogenic sulfide is the likeliest cause of deposition. Roedder (1968) has suggested that the colloform texture of schalenblende may arise through rapid deposition from a fluid supersaturated with respect to Zn. The increase in $\delta^{34}S$ values in the upper third of this sample, where the character of the sphalerite changes markedly, can be interpreted as increasing input from the

hydrothermal reservoir. There is no doubt that the deposition of the early schalenblende had ceased prior to this stage. An alternative explanation of the heavier $\delta^{34}S$ values seen in this stage is that the system gradually became closed with respect to seawater sulfate (Schwarcz and Burnie, 1973). However, we would expect that the latter process would result in a rather gradual increase in $\delta^{34}S$; this is not supported by our data, and, in any case, there is an obvious abundance of sulfide, so it seems unlikely that the system was limited by sulfur availability.

On the scale of the two hand specimens studied, there is a clear dominance of the bacteriogenic sulfur. The observed small-scale variations are therefore best explained by an episodic mixing of a hydrothermal base metal-bearing fluid with a fluid carrying reduced sulfur derived from a low temperature reservoir.

5.3. Remarks on ore genesis

Proponents of the SEDEX model for Alpine Pb-Zn deposits used the predominance of strongly negative $\delta^{34}S$ values ($< -20‰$) and the presence of fine-grained, rhythmically layered “ore sediments”, as “proof” for the syngenetic origin of the Pb-Zn ores (e.g., Schulz, 1968). However, neither of these arguments is an unequivocal proof for syn-sedimentary ore formation. Warren (2000) argues that BSR can also operate in subsurface environments down to depths of 2–2.5 km, as long as the temperature does not exceed 110 °C (e.g., BSR in enclosed pore waters). The burial depth of the Wetterstein Formation and the Raibl Group was less than 3 km until the beginning of the Late Cretaceous (100 Ma, Rantitsch, 2001). Temperature estimates, based on vitrinite reflectance and thermal modeling demonstrate that the burial temperature in the Drau Range never exceeded 110 °C (Rantitsch, 2001). BSR could therefore have been operative for several tens of millions of years in the geologic history of these deposits. Our study clearly shows that sulfur independently produced by TSR and BSR sulfur was transported by different fluids and mixed at the site of ore formation.

Formation of sedimentary ore textures is not restricted to precipitation of ore minerals on the sea floor (e.g., exhalatites); they can also form within open cavities in already lithified carbonate rocks (e.g., intra-karstic sediments, Bechstädt, 1975). At Bleiberg formation of such “internal sediments” associated with collapse breccias within meter-sized cavities has already been documented by Siegl (1956). Indeed, mixing of two fluids as demanded by our data can preferably be accomplished in lithologies with higher (secondary) porosity (fractures, veins, karst-cavities etc.) allowing directed fluid flow.

There is still no agreement on the timing of ore formation as reflected in the controversial genetic models proposed for Alpine Pb-Zn deposits. Recent Rb-Sr dating of sphalerite revealed two age groups for Bleiberg (Melcher et al., 2010): (1) A well-defined isochron age of sphalerite from various ore types and ore horizons at Bleiberg yielding 201.2 ± 1.6 Ma; (2) A less well-defined 225.2 ± 2.1 Ma isochron age based on only three samples (sphalerite and Fe-sulfides). The latter age is consistent with the Carnian stratigraphic age of the host rocks and could indicate an early mineralization stage in the Late Triassic. The well-defined ≈200 Ma age indicates that the main stage of ore formation occurred at the Triassic/Jurassic boundary and post-dated sedimentation of the carbonate host rocks by about 25 million years. This younger age would be consistent with the MVT models proposed for Alpine Pb-Zn deposits (Kuhlemann et al., 2001; Leach et al., 2003). It remains the challenge of future studies to confirm the poly-phase genesis and exact timing of ore formation of these ore deposits, especially to confirm or rule out if there is an early syngenetic (?) mineralization stage in the Late Triassic.

6. Conclusions

Samples from two different strata-bound ore horizons (Erzkalk, Maxer Bänke) in the Wetterstein Formation at Bleiberg show considerable small-scale variation in gangue mineralogy, textures, chemical composition of sphalerite and sulfur isotope composition. No strict paragenetic sequence can be established on a within-sample scale for Pb-Zn mineralization at Bleiberg precluding that it is possible to establish a uniform paragenetic sequence on the deposit or even district scale.

The two samples record opposite evolution trends in trace element chemistry and $\delta^{34}S$ values. In the Erzkalk (EHK02) an early Pb-Zn-Ba stage with a heavier hydrothermal sulfur isotopic signature and Cd-rich sphalerite predates younger BSR dominated Pb-Zn-(Fe)-F mineralization. In the sample from the Maxer Bänke horizon (Blb17) several distinct Fe-rich Zn ± (Pb)-F mineralization pulses, dominated by BSR sulfur, are followed by crystallization of Cd-rich sphalerite with heavier (hydrothermal) $\delta^{34}S$ values. The observed variations are best explained by small-scale interaction of (various) sulfur and metal carrying fluids. Such mixing of reduced sulfur from different reservoirs with major contribution from bacteriogenic derived sulfur is also a key feature of the Irish Pb-Zn deposits, which show a similar range in $\delta^{34}S$ values (Fallick et al., 2001; Wilkinson et al., 2005). Similar to the Irish deposits mixing of fluids from two reservoirs was a crucial process for ore formation in the Alpine Pb-Zn deposits: a hydrothermal fluid that interacted with the basement carrying the metals and a shallow low-temperature reservoir providing the fluids contributing sulfur derived from BSR of seawater. This light sulfur was mixed to variable extent with sulfur characterized by heavier sulfur isotope compositions, likely derived from the metal-bearing hydrothermal fluid.

Mixing of sulfur from these different sources and the metal-bearing hydrothermal fluid operated on the millimeter to centimeter scale. This is best explained by repeated short-lived mineralization pulses, a feature echoed in the textural evidence and also recorded in layered sphalerite associated with carbonate-hosted Pb-Zn mineralization elsewhere. Mixing provides an explanation for the observed sulfur isotope variations and delivers a process for ore deposition. Given the dynamism reflected by the dramatic variations across the two samples, it is therefore not surprising that a deposit-wide uniform paragenesis should prove elusive.

Acknowledgements

We thank F. Melcher and J. Lodziak (BGR Hannover) and F. Zaccarini and H. Mühlhans (Montanuniversität Leoben) for assistance with electron microprobe analyses. We are grateful to A. Butcher and W. Schwinger FEI Europe B.V. for offering the possibility to have the QEMSCAN analyses done at FEI laboratories in Brisbane, Australia and for supporting a MLA workshop at Montanuniversität Leoben. We gratefully acknowledge the support of C. Taylor and B. Davidheiser-Kroll (SUERC, UK) with sulfur isotope analyses. For providing sample material we thank O. Schulz (University of Innsbruck) and M. Götzinger (University of Vienna). Financial support of this project by a PhD grant of Montanuniversität Leoben through the Universitätszentrum Angewandte Geowissenschaften (UZAG) PhD program is acknowledged.

Appendix A. Supplementary data

Supplementary data associated with this article can be found, in the online version, at http://dx.doi.org/10.1016/j.oregeorev.2017.10.020.

References

Anderson, G.M., 1975. Precipitation of Mississippi Valley-Type ores. Econ. Geol. 70, 937–942.

Barrie, C.D., Boyce, A.J., Boyle, A.P., 2009. On the growth of colloform textures: a case study of sphalerite from the Galmoy ore body, Ireland. J. Geol. Soc. 166, 563–582. http://dx.doi.org/10.1144/0016-76492008-080.

Bechstädt, T., 1975. Lead-zinc ores dependent on cyclic sedimentation (Wetterstein-Limestone of Bleiberg-Kreuth, Carinthia, Austria). Miner. Deposita 10, 234–248.

Bechstädt, T., 1979. The lead-zinc deposit of Bleiberg-Kreuth (Carinthia, Austria): palinspastic situation, paleogeography and ore mineralisation. Verhandl. Geol. Bundesanstalt 3, 221–235.
Bischoff, J.L., Radtke, A.S., Rosenbauer, R.J., 1981. Hydrothermal alteration of graywacke by brine and seawater: roles of alteration and chloride complexing on metal solubilization at 200°C and 350°C. Econ. Geol. 76, 659–676.
Brigo, L., Kostelka, L., Omenetto, P., Schneider, H.J., Schroll, E., Schulz, O., Strucl, I., 1977. Comparative reflections on four Alpine Pb-Zn deposits. In: Klemm, D.D., Schneider, H.J. (Eds.), Time-and Strata-Bound Ore Deposits. Springer, Berlin, pp. 273–293.
Cerny, I., 1989. Die karbonatgebundenen Blei-Zink-Lagerstätten des alpinen und außeralpinen Mesozoikums. Die Bedeutung ihrer Geologie, Stratigraphie und Faziesgebundenheit für Prospektion und Bewertung. Archiv Lagerstättenforsch. Geol. Bundesanstalt 11, 5–125.
Coleman, M.L., Moore, M.P., 1978. Direct reduction of sulfates to sulfur dioxide for isotopic analysis. Analyt. Chem. 50, 1594–1595.
Coomer, P.G., Robinson, B.W., 1976. Sulphur and sulphate-oxygen isotopes and the origin of the Silvermines Deposits, Ireland. Miner. Deposita 11, 155–169.
Fallick, A.E., Ashton, J.H., Boyce, A.J., Ellam, R.M., Russell, M.J., 2001. Bacteria were responsible for the magnitude of the world-class hydrothermal base metal sulfide orebody at Navan, Ireland. Econ. Geol. 96, 885–890.
Fallick, A.E., McConville, P., Boyce, A.J., Burgess, R., Kelley, S.P., 1992. Laser microprobe stable isotope measurements on geological materials: Some experimental considerations (with special reference to ^{34}S in sulphides). Chem. Geol. Isotope Geosci. Section 101, 53–61.
Hagenguth, G., 1984. Geochemische und fazielle Untersuchungen an den Maxerbänken im Pb-Zn-Bergbau von Bleiberg-Kreuth/Kärnten. Mitt. Ges. Geol. Bergbaustud. Österr., Sonderheft 1, 110 pp.
Henjes-Kunst, E., 2014. The Pb-Zn deposits in the Drau Range (Eastern Alps, Austria/Slovenia): A multi-analytical research approach for investigation of the ore-forming mechanisms. PhD thesis. Montanuniversität Leoben, Leoben.
Henjes-Kunst, E., Boyce, A.J., Melcher, F., Raith, J.G., 2013. High-resolution sulfur isotope and trace element measurements of sphalerites from the Pb-Zn deposits of the Drau Range (Eastern Alps, Austria/Slovenia). 12th SGA Biennial Meeting, Uppsala Sweden, Conference abstracts volume 1, pp 319–322.
Herlec, U., Spangenberg, J., Lavrič, J., 2010. Sulfur isotope variations from orebody to hand-specimen scale at the Mežica lead–zinc deposit, Slovenia: a predominantly biogenic pattern. Miner. Deposita 45, 531–547.
Holler, H., 1936. Die Tektonik der Bleiberger Lagerstätte. Carinthia II, Sonderheft 7, 82 pp.
Kampschulte, A., Strauss, H., 2004. The sulfur isotopic evolution of Phanerozoic seawater based on the analysis of structurally substituted sulfate in carbonates. Chem. Geol. 204, 255–286 doi:http://dx.doi.org/10.1016/j.chemgeo.2003.11.013.
Köppel, V., 1983. Summary of lead isotope data from ore deposits of the Eastern and Southern Alps: some metallogenetic and geotectonic implications. In: Schneider, H.J. (Ed.), Mineral Deposits of the Alps and of the Alpine Epoch in Europe. Springer, Berlin, pp. 162–168.
Kucha, H., Schroll, E., Raith, J.G., Halas, S., 2010. Microbial sphalerite formation in carbonate-hosted Zn-Pb ores, Bleiberg, Austria; micro- to nanotextural and sulfur isotope evidence. Econ. Geol. 105, 1005–1023.
Kuhlemann, J., 1995. Zur Diagenese des Karawanken-Nordstammes (Österreich/Slowenien): Spättriassische, epigenetische Blei-Zink-Vererzung und mitteltertiäre, hydrothermale Karbonatzementation. Archiv Lagerstättenforsch. Geol. Bundesanstalt 18, 57–116.
Kuhlemann, J., Vennemann, T., Herlec, U., Zeeh, S., Bechstädt, T., 2001. Variations of sulfur isotopes, trace element compositions, and cathodoluminescence of Mississippi Valley-Type Pb-Zn ores from the Drau Range, Eastern Alps (Slovenia-Austria); implications for ore deposition on a regional versus microscale. Econ. Geol. 96, 1931–1941.
Leach, D.L., Bechstaedt, T., Boni, M., Zeeh, S., 2003. Triassic-hosted MVT Zn-Pb ores of Poland, Austria, Slovenia and Italy. In: Kelly, J.G., Andrew, C.J., Asthon, J.H., Boland, M.E., Earls, G., Fusciardi, L., Stanley, G. (Eds.), Europe's Major Base Metal Deposits. Irish Association for Economic Geology, Dublin, pp. 169–214.
Leach, D.L., Sangster, D.F., Kelley, K.D., Large, R.R., Garven, G., Allen, C.R., Gutzmer, J., Walters, S., 2005. Sediment-hosted lead-zinc deposits; a global perspective. In: Hedenquist, J.W., Thompson, J.F.H., Goldfarb, R.J., Richards, J.P. (Eds.), Economic Geology One Hundreth Anniversary Volume. Society of Economic Geologists, Littleton, pp. 561–607.
Machel, H.G., Krouse, H.R., Sassen, R., 1995. Products and distinguishing criteria of bacterial and thermochemical sulfate reduction. Appl. Geochem. 10, 373–389.
Melcher, F., Henjes-Kunst, F., Henjes-Kunst, E., Schneider, J., Thöni, M., 2010. Erste Rb-Sr Isotopendatierung an Sphalerit der Zn-Pb Lagerstätte Bleiberg (Kärnten), sowie Sr- und Sm-Nd-Isotopendaten von kogenetischem Karbonat und Fluorit. PANGEO 2010, Leoben. Conference abstract. J. Alpine Geol. 52, 178–180.
Ohmoto, H., Rye, R.O., 1979. Isotopes of sulfur and carbon. In: Barnes, H.L. (Ed.), Geochemistry of Hydrothermal Ore Deposits, 2nd ed. Wiley, New York, pp. 509–567.
Ohmoto, H., 1986. Stable isotope geochemistry of ore deposits. In: Valley, J.W., Taylor, Jr. H.P., O'Neil, J.R. (eds.) Stable isotopes in high temperature geological processes. Rev. Mineral. 16, 491–560.
Pfaff, K., Koenig, A., Wenzel, T., Ridley, I., Hildebrandt, L.H., Leach, D.L., Markl, G., 2011. Trace and minor element variations and sulfur isotopes in crystalline and colloform ZnS: incorporation mechanisms and implications for their genesis. Chem. Geol. 286, 118–134.
Rantitsch, 2001. Thermal history of the Drau Range (Eastern Alps). Schweiz. Mineral. Petrograph. Mitt. 81, 181–196.
Ridley, J., 2013. Ore Deposit Geology. Cambridge University Press, Cambridge.
Robinson, B.W., Kusabke, M., 1975. Quantitative preparation of sulfur dioxide, for sulfur-34/sulfur-32 analyses, from sulfides by combustion with cuprous oxide. Analyt. Chem. 47, 1179–1181.
Roedder, E., 1968. The non-colloidal origin of 'colloform' textures in sphalerite ores. Econ. Geol. 63, 451–471.
Schneider, H.J., 1964. Facies differentiation and controlling factors for the depositional lead-zinc concentration on the Ladinian geosyncline of the Eastern Alps. In: Amstutz, G.C. (ed.) Sedimentology and ore genesis. Developments in Sedimentologgy, volume 2. Elsevier, Amsterdam London New York, pp. 29–45.
Schroll, E., 1983. Geochemical characterization of the Bleiberg type and other carbonate hosted lead-zinc mineralizations. In: Schneider, H.J. (ed.), Mineral deposits of the Alps and of the Alpine epoch in Europe. Springer, Berlin Heidelberg, pp. 189–197.
Schroll, E., 1996. The Triassic carbonate-hosted Pb-Zn mineralization in the Alps (Europe): The genetic position of Bleiberg type deposits. In: Sangster, D.F. (ed.) Carbonate-hosted Pb-Zn deposits. Soc. Econ. Geol. Spec. Publ. 4, 182–194.
Schroll, E., 1996. The Triassic carbonate-hosted Pb-Zn mineralizations in the Alps (Europe). The genetic position of Bleiberg type deposits. In: Carbonate-hosted lead-zinc deposits, Spec. Pub., pp. 182–194.
Schroll, E., 2008. Blei-Zink-Lagerstätte Bleiberg. Die Geschichte ihrer Erforschung. Carinthia II Sonderheft 62. Naturwissenschaftlicher Verein für Kärnten, Klagenfurt, 286 p.
Schroll, E., Rantitsch, G., 2005. Sulphur isotope patterns from the Bleiberg deposit (Eastern Alps) and their implications for genetically affiliated lead–zinc deposits. Miner. Petrol. 84, 1–18.
Schroll, E., Schulz, O., Pak, E., 1983. Sulphur isotope distribution in the Pb-Zn-deposit Bleiberg (Carinthia; Austria). Miner. Deposita 18, 17–25.
Schulz, O., 1968. Die synsedimentäre Mineralparagenese im oberen Wettersteinkalk der Pb-Zn-Lagerstätte Bleiberg-Kreuth (Kärnten). Tschermaks Miner. Petrogr. Mitt. 12, 230–289.
Schwarcz, H.P., Burnie, S.W., 1973. Influence of sedimentary environments on sulphur isotope ratios in clastic rocks: a review. Miner. Deposita 8, 264–277.
Sicree, A.A., Barnes, H.L., 1996. Upper Mississippi Valley district ore fluid model: the role of organic complexes. Ore Geol. Rev. 11, 105–131.
Siegl, W., 1985. Bilder zur Syngenese der Bleiberger Vererzung. Archiv Lagerstättenforsch. Geol. Bundesanstalt 6, 179–182.
Siegl, W., 1956. Zur Vererzung der Pb-Zn-Lagerstätten von Bleiberg. Berg- und Hüttenmännische Monatshefte 101, 108–111.
Stanton, R.L., Russel, R.D., 1959. Anomalous leads and the emplacement of lead sulfide ores. Econ. Geol. 54, 588–607.
Wagner, T., Boyce, A.J., Fallick, A.E., 2002. Laser combustion analysis of ^{34}S of sulfosalt minerals: determination of the fractionation systematics and some crystal-chemical considerations. Geochim. Cosmochim. Acta 66, 2855–2863.
Warren, J.K., 2000. Evaporites, brines and base metals: Low-temperature ore emplacement controlled by evaporite diagenesis. Austral. J. Earth Sci. 47, 179–208.
Weber, L., 1997. Die metallogenetischen Einheiten Österreichs. Handbuch der Lagerstätten der Erze, der Industrieminerale und Energierohstoffe Österreichs. Archiv Lagerstättenforsch. 19, Geologische Bundesanstalt Wien, 607 p.
Wilkinson, J.J., Eyre, S.L., Boyce, A.J., 2005. Ore-forming processes in Irish-type carbonate-hosted Zn-Pb deposits: evidence from mineralogy, chemistry, and isotopic composition of sulfides at the Lisheen mine. Econ. Geol. 100, 63–86.
Zeeh, S., 1994. The unusual cyclicity of the Triassic (Carnian) Bleiberg facies of the Wetterstein Formation (Drau Range, Austria). Geol. Rundschau 83, 130–142.